UNIVERSITÀ DEGLI STUDI DI TORINO

Journal of the American Ceramic Society, 95, 2012

DOI: 10.1111/j.1551-2916.2012.05323.x

Hydrothermal Alteration of Glass to Chrysotile

A. Bloise,[‡,†] E. Belluso,[§,¶,k] M. Catalano,[‡‡] E. Barrese,[‡] D. Miriello,[‡] and C. Apollaro[‡]

[‡]Department of Earth Sciences, University of Calabria, Arcavacata di Rende (CS) 87036, Italy

[§]Department of Earth Sciences, University of Torino, Torino 10125, Italy

[¶]Geosciences and Geo-resources Institute (CNR), Torino section, Torino 10125, Italy

[k]NIS Centre of Excellence, Via Quarello 11, Torino 10125, Italy

[‡‡]Department of Physics, University of Calabria, Arcavacata di Rende (CS) 87036, Italy

Chrysotile fibers were synthesized from glass in hydrothermal conditions. The starting materials were first held at 1650°C and then rapidly quenched down to room temperature. The resulting glass, after the addition of mineralizing agents, was hydrothermically altered in the following conditions: temperature 300°C–400°C; pressure 100–200 MPa; time 48–480 h. X-ray powder diffraction, scanning and transmission electron microscopy were used to examine/study the starting materials and products. Cylindrical fiber morphology was prevalent, but proto-chrysotile was also detected, not entirely showing welldefined crystallinity, as revealed by electron diffraction patterns of selected areas. The mineralizing agent and chemical composition of the glass play an important role in the yield of chrysotile fibers. The effect of growth parameters on the size and abundance of chrysotile fibers is also discussed, in the light of possible recrystallization of glass obtained by thermal treatment of chrysotile-asbestos-containing materials.

I. Introduction

CHRYSOTILE is a phyllosilicate with ideal chemical formula $Mg_3Si_2O_5(OH)_4$, belonging to the serpentine group[1] and growing with asbestiform morphology (i.e., fibers with length >5 lm, width <3 lm, and aspect ratio >3). The term asbestos indicates the asbestiform varieties of five amphiboles and chrysotile minerals. Although chrysotile fibers have good technological properties,[2] if inhaled in high doses, they may cause several respiratory diseases in both humans and animals[3,4] and their use is therefore banned in many countries. However, for many years, chrysotile was used in many applications and to construct various types of artifacts (asbestos cement, tubing, reinforcing agents, fire retardants, etc.). Recently, many studies and patents have dealt with the possible disposal and re-use of chrysotile-asbestos-containing materials (ACM),[5–7] mainly through the crystal-chemical transformation induced by thermal treatment.[8–13] It has been shown that both collapse temperature and chrysotile transformation products depend on the complex mineralogical composition of ACM.[14] However, the main products of heat treatment of ACM are, in decreasing order of abundance, glass, olivine, enstatite, and diopside.[7–15] These products can be recycled to produce stoneware tile mixtures, bricks, and concrete,[8,16,17] incorporated into mortars[10] or to provide

both refractoriness and reinforcement to other materials (e.g., road beds). Finally, thermal but not recycled materials must be moved in controlled landfill. On the other hand, several researchers are studying synthesized pure and doped chrysotile fibers for possible use as nano-wires and for information on their pathological mechanisms by means of in vitro experiments. For this purpose, chrysotile fibers have been synthesized by hydrothermal treatment in various synthesis conditions and with various starting materials,[18,19] including the main products of their thermal treatment, such as forsterite,[20–25] diopside,[26] and enstatite,[27] but not glass. The present work therefore studies the experimental conditions involved in the transformation of glass into chrysotile fibers and characterizes the resulting products. Also of interest is study of the risk that, over a long period of time, the glass produced by thermal treatment of ACM may be recrystallized to chrysotile fibers by contact with percolating solutions present in landfill in which ACM has been placed.

II. Experimental Procedure (1) Starting Materials and Glass Formation

To obtain glass, the following starting materials were used: SiO_2 (granular quartz), MgO (periclase), TiO_2 (gel), and CaO (calcium oxide). To increase the reactivity between nutrients, preheating was required in a vertical furnace equipped with a Super Kanthal heating element (0°C–1700°C), with temperature controlled by PtRh–PtRh thermocouples (precision ±4°C). Granular quartz was converted into cristobalite by heating powdered SiO_2 to 1400°C; MgO powders were heated to 900°C, to eliminate hygroscopicity; TiO_2 was applied as a gel, made with $TiCl_4$ as starting material[28]; CaO was obtained by heating $CaCO_3$ powder for 24 h to 900°C to remove CO_2. All starting materials used in experiments had a purity exceeding 99%.

The molar ratio of the starting materials for two sets of glass is given below:

1. SiO_2:MgO:TiO_2:CaO = 1:1:1:1
2. SiO_2:MgO:TiO_2:CaO = 0.77:1.21:0.06:0.01

The powdered mixtures were heated in a furnace at 1650°C. The resulting melt was kept at this temperature for 48 h and then rapidly quenched down to room temperature by crucible

immersion in water. After some preliminary run tests to assess the most suitable condition to obtain glass, starting glass (1) was carried out at the same molar ratio oxides. Starting glass (2) was prepared with the same oxide wt% quantities of SiO_2, MgO, TiO_2, and CaO detected in a natural asbestiform-like serpentine mineral called carlosturanite.[29] This composition was used because the serpentine and serpentine-like mineral, carlosturanite is the richest in CaO.

This oxide, as previously tested in starting glass (1), is in fact particularly suitable as melting agent and also present in the cement-asbestos such as calcite.[8,9] The fact that glass has been obtained from starting materials (1) and (2) was confirmed by both SEM and XRPD (Figs. 1 and 2).

(2) Hydrothermal Alteration Reactions Glass fragments were cleaned by sonication in distilled water for 10 min, crushed in a mortar and sieved. The fraction of grains with size less than 0.177 mm was mixed with three types of reactants ($MgCl_2 \cdot 6H_2O$; MgO; H_2O) for four sets of reactions, given below with their weight ratios: ðaÞ glass ð1Þ þ $MgCl_2$ $6H_2O$ ðbÞ glass ð1Þ þ MgO þ $MgCl_2$ $6H_2O$ ðcÞ glass ð1Þ þ 2MgO þ H_2O ðdÞ glass ð2Þ þ H_2O

Reactants H_2O and MgO were added in stoichiometric ratios to yield chrysotile. These reactants were used because they had been previously tested in other works[26] and they are particularly suitable as mineralizing agents for chrysotile fiber growth. About 100 mg of the reaction mixtures were sealed in platinum capsules and placed in externally heated pressure vessels. Several runs of hydrothermal synthesis were carried out in these vessels (Kanthal heating wire 0°C–1000°C). Temperature was controlled by two chromel-alumel thermocouples (precision ±2.5°C, calibrated on the melting point of NaCl, i.e., 800.5) placed near the hottest portion of the device. Pressure inside the vessels was supplied through a hydrostatic circuit and continuously monitored by a Nova Swiss (Cesson, France) transducer system (accuracy ±5 bar). Hydrothermal alteration reactions were performed in the following conditions: temperature 300°C–400°C; pressure 100– 200 MPa; time 48–480 h. The capsules were then rapidly quenched in water at an estimated cooling rate of about 300°C/min. The experimental conditions are listed in Table I (glass 1) and Table II (glass 2).

(3) Characterization Techniques

The crystallinity of the starting material and the experimental run products were characterized by X-ray powder diffraction (XRPD), SEM, and TEM, with energy-dispersive X-ray spectroscopy (EDS). The XRPD patterns were obtained on a Philips PW 1730 (Philips, Eindhoven, The Netherlands) diffractometer, operating at 40 kV and 20 mA, with $Cu\kappa_a$ radiation. Scans were collected on powder samples in the range 3°–60° 2h using a step interval of 0.02° 2h, with a step counting time of 3 s. Secondary electron SEM imaging was performed on a FEI Quanta 200 (FEI, Eindhoven, The Netherlands) equipped with a field emission gun. Morphological,

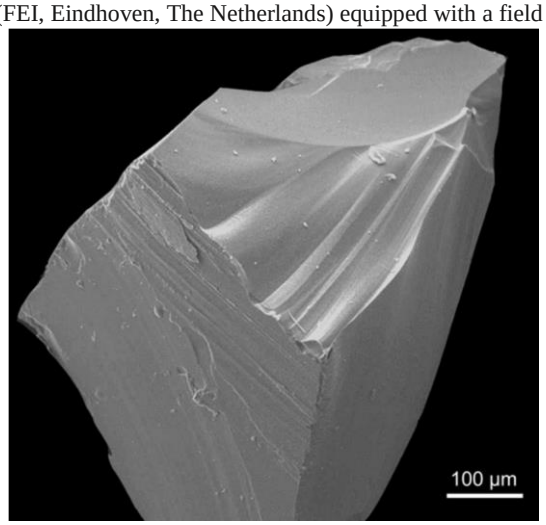

Fig. 1. Secondary electron SEM image of glass (1) fragment (starting materials 1).

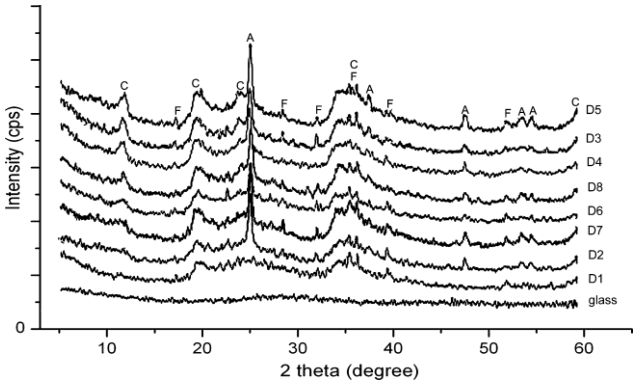

Fig. 2. XRPD pattern from starting material and products for glass (2) (Runs D1−D8, reactant d = glass (2) + H_2O). This last consists of c = chrysotile; a = anatase; f = forsterite. Peaks were assigned according to literature.

structural, and crystallinity features were examined on a TEM Philips CM12 (Philips, Eindhoven, The Netherlands), working at 120 kV with a LaB6 filament with a double tilt holder. Analytical electron microanalyses (AEM) (not shown in this study) were performed on an EDS EDAX system with Si/(Li) with a detector attached. AEM data were processed using the SUPQ software PV9800 (Philips, Eindhoven, The Netherlands) system, with default K factors to obtain normalized quantitative data. For TEM/EDS investigations, a fragment of the whole run product was gently disaggregated in isopropyl alcohol in an agate and pestle mortar and sonicated, and two drops of the resulting suspension were deposited on a copper mesh grid coated with 200 Å carbon film.

III. Results and Discussion

(1) Comparison of Products from Glass (1) and (2) The product from both sets of experiments was chrysotile. Other products, in decreasing order of abundance, were: geikielite, perovskite, calcite and brucite [glass (1)] (Table I), and anatase and forsterite [glass (2)] (Table II). In each case, as detected by TEM, starting materials in variable amounts were also present in all run products. In all runs, chrysotile fiber yields with water as mineralizing agent (reactions c, d) were always lower in abundance than those yielded by $MgCl_2 \cdot 6H_2O$ (reactions a, b). However, the yield from glass (2) (reaction d), although limited, showed that chrysotile fibers can be obtained without the aid of a mineralizing agent (reactions a, b) or other oxides such as MgO (reaction c). In glass (1) (reactions a, b, c) increasing the pressure of synthesis and time led to increasing fiber yields and sizes, whereas in glass (2) (reaction d) decreasing synthesis pressure increased chrysotile production. However, both diameter and length were greater from reactions c, d (only run D5) than reactions a, b. The formation of chrysotile fibers from glass (2) was anticipated by the formation of forsterite. This intermediate compound was easily obtained from glass (2) at 300° C (runs D1, D2), further increases in temperature causing the formation of chrysotile fibers, following the transformations observed by TEM were well described already by Yada & Iishi.[20] Instead, TEM investigations revealed that, in glass (1), chrysotile fibers do not grow through hydrothermal alteration of other intermediate products such as forsterite.

Table I. Experimental Conditions and Product List of Synthesis for Each Run for Glass (1) in Order of Decreasing Abundance as Detected by XRPD, SEM, and TEM with EDS; Fibers Length and Diameter (Averages Values from Several Measures)

Run	Reactant	T (°C)	P (MPa)	t (h)	Mineral Phases	Diameter Average (nm) (min–max)	Length Average (nm) (min–max)
C1	a	300	200	48	G > C	(5–15)	(160–625)
C2	a	300	200	96	Ctl > G > P > C		
C3	a	300	100	160	Ctl > P > C > G		
C4	a	300	200	160	Ctl > P > C > G		
C5	a	300	200	200	Ctl > C > G > P		
C6	a	300	200	288	Ctl > C > G > P		
C7	b	300	200	336	Ctl > P > C > G	(7–20)	(33–433)
C8	b	300	200	480	Ctl > P > C > G		
C9	b	300	100	360	Ctl > P > C > G		
C10	b	300	200	384	Ctl > P > G > C		
C11	b	300	100	120	Ctl > G > C > P		
C12	c	300	100	160	Brc > P > Ctl	(14–27)	(250–386)
C13	c	360	100	160	Brc > P > Ctl		
C14	c	300	200	240	P > Ctl > Brc		

a = glass (1) + $MgCl_2 \cdot 6H_2O$; b = glass (1) + MgO + $MgCl_2 \cdot 6H_2O$; c = glass (1) + 2MgO + H_2O. Ctl = chrysotile; Brc = brucite; G = geikielite; C = calcite; P = perovskite.

Table II. Expermental Conditions and Products of Synthesis for Each Run for Glass (2) in Order of Decreasing Abundance as Detected by XRPD, SEM, and TEM-EDS

Run	Reactant	T (°C)	P (MPa)	t (h)	Mineral Phases	Diameter Average (nm) (min–max)	Length Average (nm) (min–max)
D1	d	300	100	160	Fo	–	–
D2	d	300	200	160	A > Fo	–	–
D3	d	330	100	320	A > pC > Fo	–	–
D4	d	330	100	160	A > Fo > pC	–	–
D5	d	360	100	160	pC > Ctl > A > Fo	(115–450)	(9–85)
D6	d	360	200	160	A > Fo > pC	–	–
D7	d	400	100	160	Fo > pC > A	–	–
D8	d	400	200	160	Fo > A > pC	–	–

= glass (2) + H_2O. Ctl = chrysotile; A = anatase; Fo = forsterite; pC = proto-chrysotile.

Results for Glass (1)

With the glass from glass (1), secondary products occurred rapidly, with the formation of calcite and geikielite ($MgTiO_3$) after 48 h of reaction. After 96 h, chrysotile and perovskite ($CaTiO_3$) also appeared. An increase in the time of hydrothermal alteration of glass (1) (reactant a), at constant temperature and pressure (300°C, 200 MPa), produced larger fibers. With $MgCl_2 \cdot 6H_2O$ as reactant (Table I; reactants a, b), chrysotile crystallized as the main phase. The most abundant production of chrysotile was obtained with reactant b after a long period (480 h, 200 MPa, 300°C, run C8; Table I). As regards the different set of reactions (Table I, runs C1–C14) glass composition does not seem to be crucial as mineralizing agent (i.e., $MgCl_2 \cdot 6H_2O$ or water) in producing greater abundances of chrysotile fibers. When distilled H_2O (reagent c) was used instead of $MgCl_2 \cdot 6H_2O$ (reagents a, b) to alter glass (1), chrysotile yield decreased considerably, but an increase in both pressure and reaction time had the opposite effect (run C14). However, with $MgCl_2 \cdot 6H_2O$ as reactant (reactant a, b), fiber diameter and length decreased with respect to chrysotile fibers obtained with distilled H_2O as reagent (Table I; reagent c). TEM investigations showed that fibers obtained with reactant a (Fig. 3) had an average diameter smaller than those obtained with either reactants b or c (Figs. 4 and 5; Table I]. Only distilled water as reactant in glass (1) turned out to provide the best synthesis conditions for more abundant chrysotile, which was obtained at 300°C and 200 MPa, with a reaction time of 240 h (run C14). As regards morphology, in all sets of runs, fibers mostly showed the classical cylindrical morphology, but cone-in-cone shape was also detected. In all

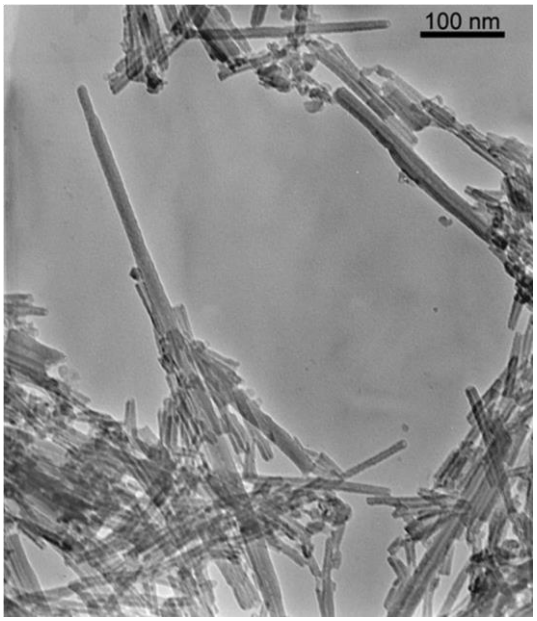

Fig. 3. Transmission electron micrograph of chrysotile fibers, as seen in the plane of fiber axis, from run C4 (300°C, 200 MPa, 160 h), reactant a = glass (1) + $MgCl_2 \cdot 6H_2O$.

runs with glass (1) (see Table I), fibers showed empty cores throughout their length, some cores being poorly shaped and partially filled.

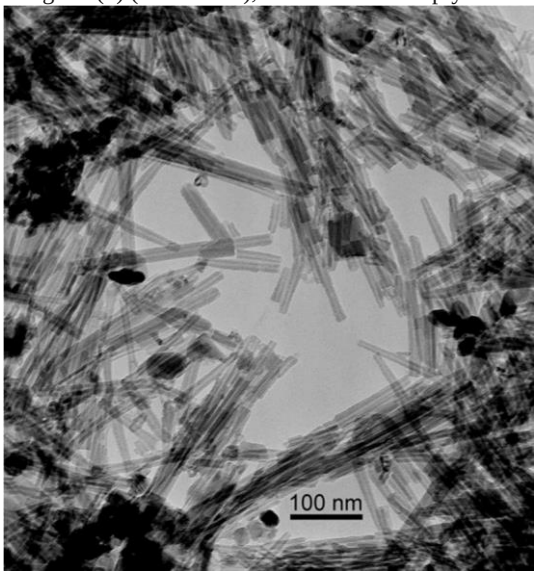

Fig. 4. Transmission electron micrograph of chrysotile fibers, as seen in the plane of fiber axis, from run C8 (300°C, 200 MPa, 480 h), reactant b = glass (1) + MgO + $MgCl_2 \cdot 6H_2O$.

(3) Results for Glass (2)

Subjecting glass (2) to various hydrothermal conditions, as shown by the XRPD patterns of Fig. 2, chrysotile was yielded at 400°C (100 MPa, 160h; run D7), although forsterite and anatase had already formed at 300°C (200 MPa, 160 h; run D2). At 400°C, a decrease in reaction pressure from 200 MPa (run D8) to 100 MPa (run D7) slightly improved the amount of chrysotile produced. The XRPD reflection of the newly formed chrysotile became sharper with decreasing temperature from 400°C (Run D7) to 360°C (Run D5), corresponding to increases in chrysotile fiber size and abundance. However, when the temperature was decreased from 360°C (Run D5) to 330°C (Run D4) and then to 300°C (Run D2), there was no further increase in chrysotile yield. TEM micrograph (Fig. 6) shows the initial stages of serpentinization (run D7). After 160 h of hydrothermal reaction at 400°C and 100 MPa (run D7), the main phase crystallizing as particles was forsterite, while chrysotile began to grow

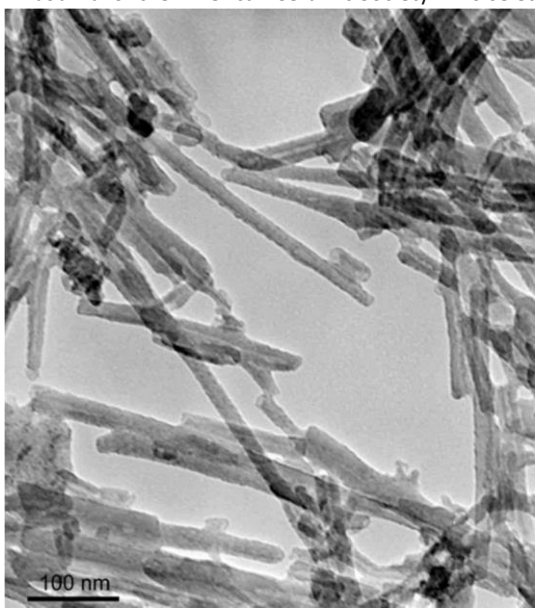

Fig. 5. Transmission electron micrograph of chrysotile fibers, as seen in the plane of fiber axis, from run C12 (300°C, 100 MPa, 160 h), reactant c = glass (1) + 2MgO + H_2O.

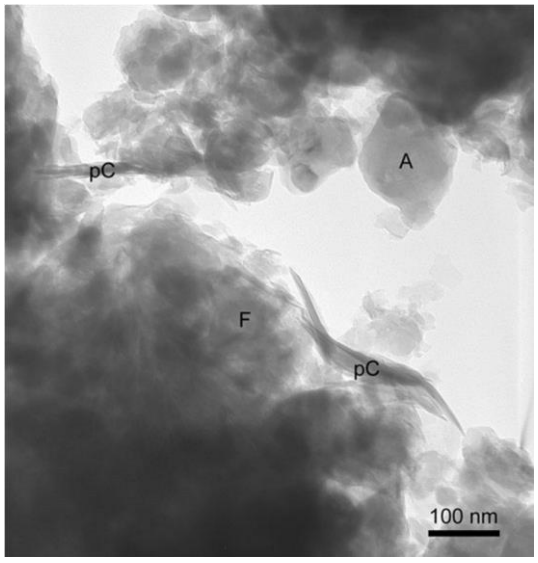

Fig. 6. Transmission electron micrograph of initial stage of chrysotile formation, from run D7 (400°C, 100 MPa, 160 h), reactant d = glass (2) + H_2O. pC = proto-chrysotile, F = forsterite, A = anatase.

from the surface of forsterite particles (Fig. 6). The surface seemed to peel off in many layers. These layers were partially wrapped and in some places appeared to be thicker, indicating greater curling of the T–O chrysotile layers. However, no chrysotile showing the classical cylindrical morphology with empty cores developed throughout the fiber length (run D7). In this stage, chrysotile grew with exclusively proto-chrysotile morphology[30] and exhibited poor crystallinity, as confirmed by SAED investigations. Proto-chrysotile morphology is the precursor of the cylindrical morphology of chrysotile, as already extensively described by Yada & Iishi[20] and Muriel et al.[30] However, the decrease of the temperature to 360°C (run D5) led to a decrease in the amount of proto-chrysotile, while the growth of the classical cylindrical chrysotile appeared. In comparison with other runs, in run D5 the chrysotile layers were thicker along the forsterite relict edges

Fig. 7. Transmission electron micrograph of chrysotile layers via curling formed on the edge of forsterite relict, from run D5 (360°C, 100 MPa, 160 h), reactant d = glass (2) + H_2O.

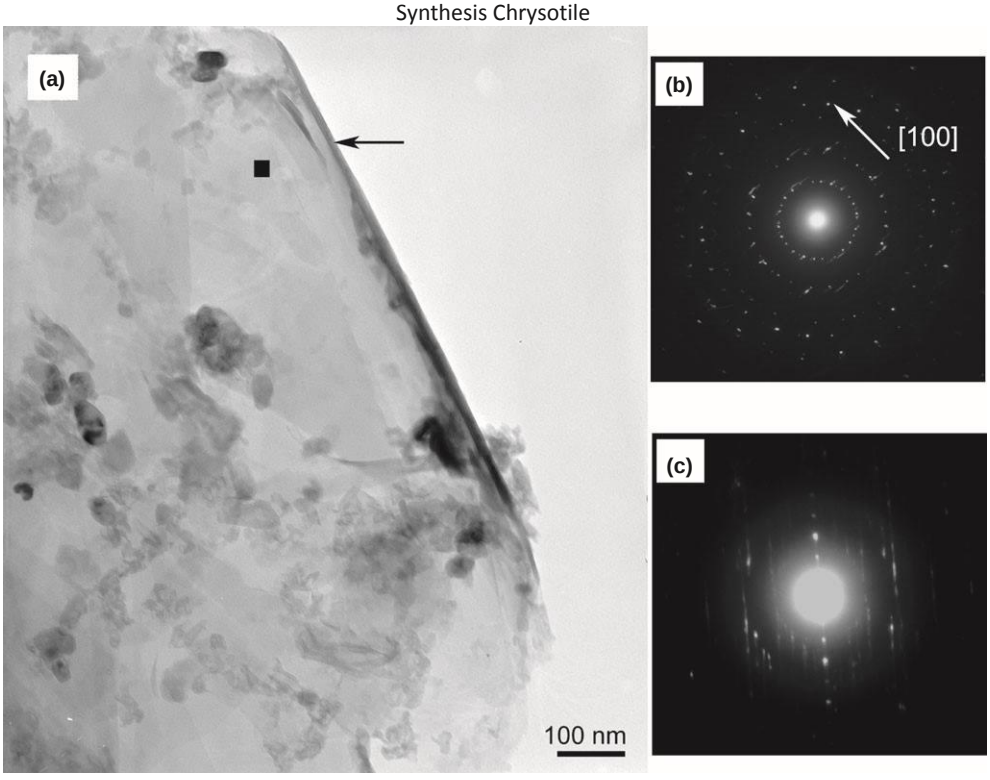

Fig. 8. Chrysotile via curling of the layers formed on the edge of forsterite relict, from run D5 (360°C, 100 MPa, 160 h), reactant d = glass (2) + H_2O. (a) Transmission electron micrograph, (b) electron diffraction pattern of chrysotile via curling indicated by arrow as seen on the fiber axis plane (c) electron diffraction pattern of forsterite relict, carried out on the point indicated by full black square in transmission electron micrograph a).

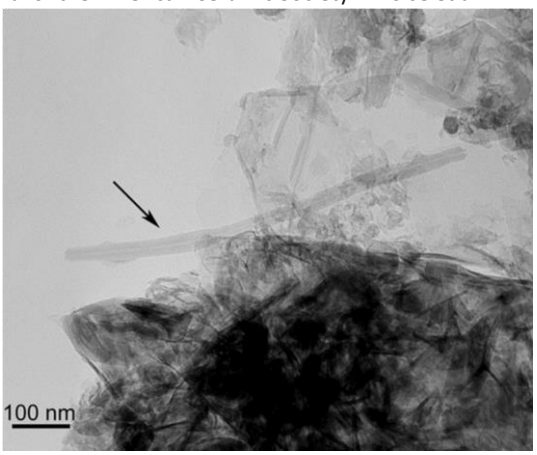

Fig. 9. Transmission electron micrograph of chrysotile fiber (indicated by arrow) and layers via curling, from run D5 (360°C, 100 MPa, 160 h), reactant d = glass (2) + H_2O.

and the curling of the layers became more evident [Figs. 7 and 8(a)].

Figure 8(c) shows a SAED micrograph from the surface of the olivine relict and from the edge, where the membrane is being rolled up to form chrysotile fibers [Fig. 8(b)]. As this is a phase of transformation from forsterite to chrysotile, both SAED micrographs [Figs. 8(c) and (b)] show structural disorder. However, in Fig. 8(b), the typical splitting of the diffraction spots of the chrysotile fibers begins to appear, due to the cylindrical crystal lattice lying along layer lines. Lastly, as the XRPD pattern shows (Fig. 2), in run D5 crystallinity increases and the classical cylindrical morphology with a hollow central core running longitudinally along the fiber axis can be observed (Fig. 9), bent owing to interaction with the electron beam. However, TEM showed that only a few

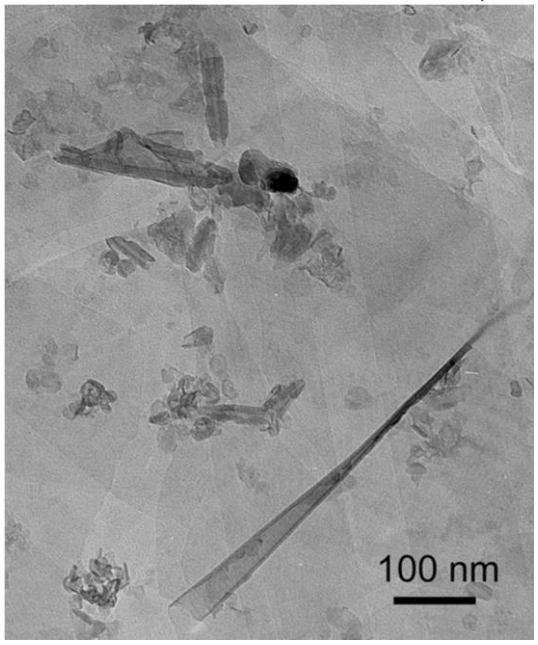

Fig. 10. Transmission electron micrograph of proto-chrysotile fibers from run D5 (360°C, 100 MPa, 160 h), reactant d = glass (2) + H_2O.

fibers have the typical cylindrical shape, proto-chrysotile being the most abundant morphology (Fig. 10). Some of the fibers do not have empty cores all the way along their axes, indicating the absence of core voids.

IV. Conclusions

Chrysotile fibers were synthesized from glass in hydrothermal conditions. On the whole, the best conditions for more abundant and greater lengthening of fibers were temperature at 300°C, pressure at 200 MPa, long reaction times (480 or 240 h) for glass (1), and 360°C, 100 MPa, and 160 h for glass (2). Chrysotile fibers were easily obtained in large quantities from glass (1) but only in small amounts from glass (2), in which the lower quantity was probably due to the formation of intermediate products such as forsterite. Growth parameters (temperature, pressure, reaction time) required to obtain chrysotile fibers from glass (2) were very similar to those used to alter forsterite by other authors. Conversely, chrysotile formation was increased by treating glass (1) with a mineralizing agent such as $MgCl_2 \cdot 6H_2O$ or MgO, probably because the formation of forsterite was inhibited by the mineralizing agent. With $MgCl_2 \cdot 6H_2O$ as mineralizing agent, more abundant production of chrysotile fibers was achieved, although they could also be obtained by altering glass (2) with distilled water only. It is concluded that the effect of mineralizing agent

($MgCl_2 \cdot 6H_2O$ or MgO) prevailed over growth parameters as regards increased chrysotile fiber production, although prolonged reaction times led to larger fiber size.

In the light of these results also glass produced as a result of thermal treatment of ACM containing chrysotile, when placed in landfills, owing to possible long-term increases in temperature and pressure and contact with percolating solutions (i.e., natural water) can probably be hydrothermally altered and recrystallized to chrysotile. Instead,as regards recycling ACM into inert products (bricks, tiles, ceramics), the possibility of their recrystallization into chrysotile fibers in ambient conditions is probably remote. Further experimental runs are continuing, with the aim of recrystallizing chrysotile fibers from glass obtained by melting natural chrysotile fibers or ACM.

References

1 W. A. Deer, R. A. Howie, and J. Zussman, Rock-Forming Minerals Layered Silicates Excluding Micas and Clay Minerals, Vol. 3B. The Geological Society, London, (2009).

2 K. Chernoutsan, V. Dneprovskii, S. Gavrilov, V. Gusev, E. Muljarov, S. Romanov, A. Syrnicov, O. Shaligina, and E. Zhukov, "Linear and Nonlinear Optical Properties of Excitons in Semiconductor-Dielectric Quantum Wires," Physica E, 15, 111–7 (2002).

3 M. E. Gunter, E. Belluso, and A. Mottana, "Amphiboles: Environmental and Health Concerns"; pp. 453–516 in Amphiboles: Crystal Chemistry, Occurrence, and Health Issues, Vol. 67, Reviews in Mineralogy & Geochemistry, Edited by C. F. Hawthorne, R. Oberti, G. Della Ventura and A. Mottana.
Mineralogical Soc. America Geochemical Soc., Chantilly, VA, 2007.

4 G. D. Guthrie and B. T. Mossman, "Merging the Geological and Biological Science an Integrated Approach to Mineral Induced Pulmonary Disease"; pp. 1–5 in Health Effects of Mineral Dusts, Vol. 28, Reviews in Mineralogy & Geochemistry. Edited by G. D. Guthrie and B. T. Mossman. Mineralogical Soc. America Geochemical Soc., Chelsea, MI, 1993.

5 P. Plescia, D. Gizzi, S. Benedetti, L. Camilucci, C. Fanizza, P. De Simone, and F. Paglietti, "Mechanochemical Treatment to Recycling Asbestos-Containing Waste," Waste Manage., 23, 209–18 (2003).

6 S. E. Favero-Longo, D. Castelli, B. Fubini, and R. Piervittori, "Lichens on Asbestos-Cement Roofs: Bioweathering and Biocovering Effects," J. Hazard.
Mater., 162, 1300–8 (2009).

7 K. Anastasiadou, D. Axiotis, and E. Gidarakos, "Hydrothermal Conversion of Chrysotile Asbestos Using Near Supercritical Conditions," J. Hazard.
Mater., 179, 926–32 (2010).

8 A. F. Gualtieri, C. Cavenati, I. Zanatto, M. Meloni, G. Elmi, and M. Lassinantti Gualtieri, "The Transformation Sequence of Cement–Asbestos Slates up to 1200°C and Safe Recycling of the Reaction Product in Stoneware Tile Mixtures," J. Hazard. Mater., 152, 563–70 (2008).

9 F. Dellisanti, P. L. Rossi, and G. Valdre` , "Remediation of Asbestos Containing Materials by Joule Heating Vitrification Performed in a Pre-Pilot Apparatus," Int. J. Miner. Process., 91, 61–7 (2009).

10 Y. Yvon and P. Sharrock, "Characterization of Thermochemical Inactivation of Asbestos Containing Wastes and Recycling the Mineral Residues in Cement Products," Waste Biomass Valor., 2, 169–81 (2011).

11 D. N. Boccaccini, C. Leonelli, M. R. Rivasi, M. Romagnoli, P. Veronesi, G. C. Pellacani, and A. R. Boccaccini, "Recycling of Microwave Inertised Asbestos Containing Waste in Refractory Materials," J. Eur. Ceram. Soc., 27, 1855–8 (2007).

12 P. A. Candela, C. D. Crummett, D. J. Earnest, M. R. Frank, and A. G. Wylie, "Low-Pressure Decomposition of Chrysotile as a Function of Time and Temperature," Am. Mineral., 92 [10] 1704–13 (2007).

13 C. Leonelli, P. Veronesi, D. N. Boccaccini, M. R. Rivasi, L. Barbieri, F. Andreola, I. Lancellotti, D. Rabitti, and G. C. Pellacani, "Microwave Thermal Inertisation of Asbestos Containing Waste and its Recycling in Traditional Ceramics," J. Hazard. Mater., 135, 149–55 (2006).

14 F. Dellisanti, V. Minguzzi, and N. Morandi, "Experimental Results from Thermal Treatment of Asbestos Cantaining Materials," GeoActa, 1, 61–70 (2002).

15 C. Giacobbe, A. F. Gualtieri, S. Quartieri, C. Rinaudo, M. Allegrina, and G. B. Andreozzi, "Spectroscopic Study of the Product of Thermal Transformation on Chrysotile-Asbestos Containing Materials," Eur. J. Mineral., 22 [4] 535–46 (2010).

16 A. F. Gualtieri, C. Giacobbe, L. Sardisco, M. Saraceno, M. L. Gualtieri, G. Lusvardi, C. Cavenati, and I. Zanatto, "Recycling of the Product of Thermal Inertization of Cement-Asbestos for Various Industrial Applications," Waste Manag., 31 [1] 91–100 (2011).

17 A. F. Gualtieri and M. Boccaletti, "Recycling of the Product of Thermal Inertization of Cement-Asbestos for the Production of Concrete," Construct.
Build. Mater., 25, 3561–9 (2011).

18 N. Roveri, G. Falini, E. Foresti, G. Fracasso, I. G. Lesci, and P. Sabatino, "Geoinspired Synthetic Chrysotile Nanotubes," J. Mater. Res., 21 [11] 2711–25 (2006).

19 G. Falini, E. Foresti, G. Lesci, and N. Roveri, "Structural and Morphological Characterization of Synthetic Chrysotile Single Crystals," Chem. Commun., 14, 1512–3 (2002).

20 K. Yada and K. Iishi, "Growth and Microstructure of Synthetic Chrysotile," Am. Mineral., 62, 958–65 (1977).

21 C. Normand, A. E. W. Jones, F. R. Martin, and H. Vali, "Hydrothermal Alteration of Olivine in a Flow-Through Autoclave: Nucleation and Growth of Serpentine Phases," Am. Mineral., 87, 1699–709 (2002).

22 A. Bloise, E. Barrese, and C. Apollaro, "Hydrothermal Alteration of TiDoped Forsterite to Chrysotile and Characterization of the Resulting Chrysotile Fibers," N. Jb. Miner. Mh., 185 [3] 297–304 (2009).

23 A. Bloise, E. Belluso, E. Fornero, C. Rinaudo, E. Barrese, and S. Capella, "Influence of Synthesis Condition on Growth of Ni-Doped Chrysotile," Microporous Mesoporous Mater., 132, 239–45 (2010).

24 A. Bloise, E. Belluso, E. Barrese, D. Miriello, and C. Apollaro, "Synthesis of Fe-Doped Chrysotile and Characterization of the Resulting Chrysotile Fibers," Cryst. Res. Technol., 44 [6] 590–6 (2009).

25 A. Filippidis, "Experimental Study of the Serpentinization of Mg-Fe-Ni Olivine in the Presence of Sulfur," Can. Mineral., 20, 567–74 (1982).

26 E. Barrese, E. Belluso, and F. Abbona, "On the Transformation of Synthetic Diopside Into Chrysotile," Eur. J. Mineral., 9, 83–7 (1997).

27 E. N. Korytkova, A. V. Maslov, L. N. Pivovarova, I. A. Drozdova, and V. V. Gusarov, "Formation of $Mg_3Si_2O_5(OH)_4$ Nanotubes Under Hydrothermal Conditions," Glass Phys. Chem., 30 [1] 51–5 (2004).

28 Yu. V. Kolen'ko, A. A. Burukhin, B. R. Churagulov, and N. N. Oleinikov, "Phase Composition of Nanocrystalline Titania Synthesized Under Hydrothermal Conditions from Different Titanyl Compounds," Inorg. Mater., 40, 822–8 (2004).

29 R. Compagnoni, G. Ferraris, and M. Mellini, "Carlosturanite, a New Asbestiform R-Forming Silicate from Val Varaita, Italy," Am. Mineral., 70, 767–72 (1985).

30 A. Muriel, O. Grauby, A. Baronnet, and M. Mun˜ oz, "Occurence, Composition and Growth of Polyhedral Serpentine," Eur. J. Mineral., 20 [2] 159–71
(2008).h